Phase coexistence in [111] electric-field-cooled 0.7Pb $(Mg_{1/3}Nb_{2/3})O_3$–$0.3PbTiO_3$ crystals

2007 J. Phys.: Condens. Matter 19 246224

(http://iopscience.iop.org/0953-8984/19/24/246224)

IOP PUBLISHING JOURNAL OF PHYSICS: CONDENSED MATTER

J. Phys.: Condens. Matter **19** (2007) 246224 (9pp) doi:10.1088/0953-8984/19/24/246224

Phase coexistence in [111] electric-field-cooled $0.7Pb(Mg_{1/3}Nb_{2/3})O_3$–$0.3PbTiO_3$ crystals

V Yu Topolov[1], Hu Cao[2] and D Viehland[2]

[1] Department of Physics, Southern Federal University, Zorge Street 5, 344090 Rostov-on-Don, Russia
[2] Department of Materials Science and Engineering, Virginia Tech, Blacksburg, VA 24061, USA

E-mail: topolov@phys.rsu.ru

Received 7 March 2007, in final form 8 May 2007
Published 30 May 2007
Online at stacks.iop.org/JPhysCM/19/246224

Abstract

Features of phase coexistence in polydomain $0.7Pb(Mg_{1/3}Nb_{2/3})O_3$–$0.3PbTiO_3$ crystals cooled under an applied [111] electric field $\boldsymbol{E}$ have been investigated. A sequence of ferroelectric phases as well as the elastic matching between coexisting phases in heterophase states has been analysed for cases where the angle between the spontaneous polarization vector of each domain type and the applied $\boldsymbol{E}$ vector remains equal in each ferroelectric phase. This analysis is based on a method that involves distortion matrices of the polydomain phases and invariants of interfaces regarded as quadric surfaces separating the phases. Results are represented in a system of diagrams linking domain states and interfaces at first-order phase transitions observed in [111] field-cooled $0.7Pb(Mg_{1/3}Nb_{2/3})O_3$–$0.3PbTiO_3$ crystals. A 'fine' structure of the domain state–interface diagrams related to tetragonal–orthorhombic phase coexistence has been revealed. It has been shown that conditions for complete stress relaxation in different heterophase states are achieved for a phase sequence of cubic $\rightarrow$ polydomain tetragonal $\rightarrow$ near single-domain orthorhombic $\rightarrow$ single-domain monoclinic of the B type.

1. Introduction

Perovskite-type relaxor–ferroelectric solid solutions, such as $(1-x)Pb(Mg_{1/3}Nb_{2/3})O_3$–$xPbTiO_3$ (PMN–xPT), are of interest due to significantly enhanced electromechanical properties [1], the presence of unique intermediate (or 'bridging') phases [2–4], and a 'fragile' phase stability that depends on the crystal history [5]. Recent investigations [5–8] of electric-field-cooled PMN–xPT crystals have shown that the orientation of an externally applied electric field ($\boldsymbol{E}$) considerably influences the phase transformational sequence on cooling, in particular for compositions close to the morphotropic phase boundary ($0.30 \leqslant x \leqslant 0.35$). For example, the following phase sequences have been reported for PMN–0.30PT crystals

on cooling: cubic (C) $Pm3m \rightarrow$ tetragonal (T) $P4mm \rightarrow$ rhombohedral (R) $R3m$ for $E = 0$ [6], C $\rightarrow$ T $\rightarrow$ monoclinic C (M_C) $\rightarrow$ monoclinic A (M_A) for $E > 0 \parallel [001]$ [6], and C $\rightarrow$ T $\rightarrow$ orthorhombic (O) $\rightarrow$ monoclinic B (M_B) for $E > 0 \parallel [110]$ [6] or $E > 0 \parallel [111]$ [8]; here the crystallographic directions $[hkl]$ are written with respect to the pseudo-cubic perovskite unit-cell axes. The fact that a crystal can be R, T, M_A, M_B, M_C, or O demonstrates that these phases are nearly thermodynamically degenerate, i.e., the free energy landscape is abnormally flat.

Heterophase states have also been reported to exist in intermediate temperature ranges about various transitional steps in the phase transformational sequence of PMN–xPT crystals. The role of domain (twin) structures on stabilizing heterophase states by stress accommodation in PMN–xPT ($x = 0.30$ and 0.35) has been analysed for $\boldsymbol{E} \parallel [001]$ and $\boldsymbol{E} \parallel [110]$ [9]. Also, quite recently, unit-cell parameters of field-cooled PMN–0.30PT crystals were reported for $\boldsymbol{E} = 2$ kV cm$^{-1} \parallel [111]$ [8]. Using these lattice parameter data for PMN–0.30PT, it would be possible to extend the microelastic approach to the stabilization of heterophase states under $\boldsymbol{E} \parallel [111]$. In this work we present such an analysis of domain (twin) structures for T, O, and M_B phases in various heterophase states (within which phases can coexist) for PMN–0.30PT crystals cooled under $\boldsymbol{E} \parallel [111]$.

2. Polydomain phases and interfaces

A study of the formation of domain (twin) structures in ferroelectric crystals is usually carried out in terms of crystallographic [10–12] and thermodynamic [11, 13] theories, in which lowering of the elastic energy for a heterophase crystal has been found to result in the formation of equilibrium domain structures. As a consequence, the new polydomain phase retains its coherency with the parent phase, and the interfaces separating coexisting phases are, on average, undistorted [14]. Metrat [12] developed a crystallographic theory [14] to describe complex domain structures and their elastic matching at first-order phase transitions in ferroelectric and related crystals. The method used in our present work generalizes Metrat's concepts [12], enabling us to classify possible interfaces at various volume fractions of different domain types and to find optimal conditions for complete stress accommodation in heterophase states. Implementation of this method requires three stages, as follows.

The first stage is concerned with a determination of domain-type orientations and their distortion matrices in each ferroelectric phase. The distortion matrices of the polydomain phases are written as functions of volume fractions of the domain types. In the second stage, an analysis of elastic matching of the coexisting phases is performed. Finally, in the third stage, diagrams linking possible domain states in the coexisting phases and the interfaces between these phases are determined for various volume fractions of different domain types.

We begin describing the different heterophase states by considering a stress-free crystal undergoing a first-order phase transition on electric-field cooling. A schematic diagram of the possible non-180° domain orientations in a perovskite unit cell is given in figure 1. This figure suggests that $\boldsymbol{E} \parallel [111]$ would promote the formation of three non-180° domain types, having equivalent orientations relative to $\boldsymbol{E}$ in the T, O, or M_B phase. It is noteworthy that the angles between the spontaneous polarization and electric-field vectors in the respective phases are $\psi_T(\boldsymbol{P}_{Tj} \hat{} \boldsymbol{E}) = \cos^{-1}(1/\sqrt{3})$, $\psi_O(\boldsymbol{P}_{Oj} \hat{} \boldsymbol{E}) = \cos^{-1}(\sqrt{2/3})$, and $\psi_{M_B}(\boldsymbol{P}_{M_Bj} \hat{} \boldsymbol{E}) = \cos^{-1}[(p+2)/\sqrt{3(p^2+2)}]$ for $j = 1, 2$, and 3 and $0 < p < 1$. These angles do not depend on the domain orientation in their respective phase: such independence of ψ on $\boldsymbol{E}$ is unattainable for $\boldsymbol{E} \parallel [001]$ or $\boldsymbol{E} \parallel [110]$. For the lamellar type of domain (twin) structures observed in PMN–xPT [4, 15], the domain walls can be assumed to be stress free [16]. The perovskite

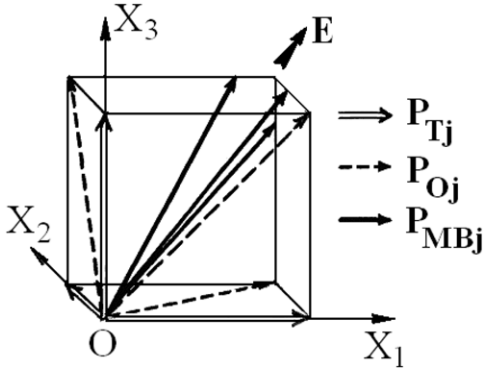

Figure 1. Schematic drawing of non-180° domain orientations in a perovskite unit cell. The spontaneous polarization vectors $\boldsymbol{P}_{\mathrm{T}j}$, $\boldsymbol{P}_{\mathrm{O}j}$, and $\boldsymbol{P}_{\mathrm{M_B}j}$ are related to the domains of the T, O, and $\mathrm{M_B}$ phases, respectively, for $j = 1$, 2, or 3. The electric field vector was applied as $\boldsymbol{E} \parallel [111]$. Coordinate axes OX_k are parallel to the perovskite unit-cell axes: i.e., $OX_1 \parallel [100]$, $OX_2 \parallel [010]$, and $OX_3 \parallel [001]$.

unit-cell vectors $(\boldsymbol{a}_j, \boldsymbol{b}_j, \boldsymbol{c}_j)$ of individual domain types in each ferroelectric phase are arranged by taking into account the rotation angles and unit-cell shear angles [3], approximately along the following crystallographic directions: ([100], [010], [001]) for $j = 1$, ([001], [100], [010]) for $j = 2$, and ([010], [001], [100]) for $j = 3$. Following the matrix method [3, 12, 17], a distortion matrix is written with respect to the coordinate axes shown in figure 1.

The distortion matrices of the polydomain T, O, and $\mathrm{M_B}$ phases are then respectively

$$\begin{aligned}\|N_{kl}^{(\mathrm{T})}\| = {} & m_{\mathrm{T}}\begin{pmatrix}\varepsilon_a & 0 & 0\\ 0 & \varepsilon_a & 0\\ 0 & 0 & \varepsilon_c\end{pmatrix} + n_{\mathrm{T}}\begin{pmatrix}1 & 0 & 0\\ 0 & \cos\varphi_{\mathrm{T}} & \sin\varphi_{\mathrm{T}}\\ 0 & -\sin\varphi_{\mathrm{T}} & \cos\varphi_{\mathrm{T}}\end{pmatrix}\begin{pmatrix}\varepsilon_a & 0 & 0\\ 0 & \varepsilon_c & 0\\ 0 & 0 & \varepsilon_a\end{pmatrix}\\ & + (1 - m_{\mathrm{T}} - n_{\mathrm{T}})\begin{pmatrix}\cos\varphi_{\mathrm{T}} & 0 & -\sin\varphi_{\mathrm{T}}\\ 0 & 1 & 0\\ \sin\varphi_{\mathrm{T}} & 0 & \cos\varphi_{\mathrm{T}}\end{pmatrix}\begin{pmatrix}\varepsilon_c & 0 & 0\\ 0 & \varepsilon_a & 0\\ 0 & 0 & \varepsilon_a\end{pmatrix} \qquad (1a)\end{aligned}$$

$$\begin{aligned}\|N_{kl}^{(\mathrm{O})}\| = {} & m_{\mathrm{O}}\begin{pmatrix}\eta_a & 0 & 0\\ 0 & \eta_a & 0\\ 0 & 0 & \eta_c\end{pmatrix} + n_{\mathrm{O}}\begin{pmatrix}1 & 0 & 0\\ 0 & \cos\varphi_{\mathrm{O}} & \sin\varphi_{\mathrm{O}}\\ 0 & -\sin\varphi_{\mathrm{O}} & \cos\varphi_{\mathrm{O}}\end{pmatrix}\begin{pmatrix}\eta_a & 0 & 0\\ 0 & \eta_c & 0\\ 0 & 0 & \eta_a\end{pmatrix}\\ & + (1 - m_{\mathrm{O}} - n_{\mathrm{O}})\begin{pmatrix}\cos\varphi_{\mathrm{O}} & 0 & -\sin\varphi_{\mathrm{O}}\\ 0 & 1 & 0\\ \sin\varphi_{\mathrm{O}} & 0 & \cos\varphi_{\mathrm{O}}\end{pmatrix}\begin{pmatrix}\eta_c & 0 & 0\\ 0 & \eta_a & 0\\ 0 & 0 & \eta_a\end{pmatrix} \qquad (1b)\end{aligned}$$

and

$$\begin{aligned}\|N_{kl}^{(\mathrm{M_B})}\| = {} & m_{\mathrm{M_B}}\begin{pmatrix}\lambda_a & \lambda & 0\\ \lambda & \lambda_a & 0\\ 0 & 0 & \lambda_c\end{pmatrix} + n_{\mathrm{M_B}}\begin{pmatrix}1 & 0 & 0\\ 0 & \cos\varphi_{\mathrm{M_B}} & \sin\varphi_{\mathrm{M_B}}\\ 0 & -\sin\varphi_{\mathrm{M_B}} & \cos\varphi_{\mathrm{M_B}}\end{pmatrix}\begin{pmatrix}\lambda_a & 0 & \lambda\\ 0 & \lambda_c & 0\\ \lambda & 0 & \lambda_a\end{pmatrix}\\ & + (1 - m_{\mathrm{M_B}} - n_{\mathrm{M_B}})\begin{pmatrix}\cos\varphi_{\mathrm{M_B}} & 0 & -\sin\varphi_{\mathrm{M_B}}\\ 0 & 1 & 0\\ \sin\varphi_{\mathrm{M_B}} & 0 & \cos\varphi_{\mathrm{M_B}}\end{pmatrix}\begin{pmatrix}\lambda_c & 0 & 0\\ 0 & \lambda_a & \lambda\\ 0 & \lambda & \lambda_a\end{pmatrix}. \qquad (1c)\end{aligned}$$

In equation (1*a*), m_{T} and n_{T} are the volume fractions of the first and second domain types, and ε_a and ε_c are the unit-cell distortions expressed in terms of the unit-cell parameters of the T phase [3]. The angle $\varphi_{\mathrm{T}} = \cos^{-1}[2\varepsilon_a\varepsilon_c/(\varepsilon_a^2 + \varepsilon_c^2)]$ is introduced to account for possible rotations of the crystallographic axes between adjacent domains [3, 12]. The volume fractions m_{T} and n_{T} obey the condition $0 \leqslant m_{\mathrm{T}} + n_{\mathrm{T}} \leqslant 1$. Similar inequalities, $0 \leqslant m_{\mathrm{O}} + n_{\mathrm{O}} \leqslant 1$ and $0 \leqslant m_{\mathrm{M_B}} + n_{\mathrm{M_B}} \leqslant 1$, are then introduced for the volume fractions of the domains in the

O (m_{O} and n_{O}) and $\mathrm{M_B}$ ($m_{\mathrm{M_B}}$ and $n_{\mathrm{M_B}}$) phases. The rotation angles $\varphi_{\mathrm{O}} = \cos^{-1}[2\eta_a\eta_c/(\eta_a^2 + \eta_c^2)]$ and $\varphi_{\mathrm{M_B}} = \cos^{-1}[2\lambda_a\lambda_c/(\lambda_a^2 + \lambda_c^2)]$ from equations (1*b*) and (1*c*) are defined by analogy to φ_{T}. Also, note that the distortion matrix of the paraelectric C phase, $\|N_{kl}^{(C)}\|$, is the identity 3×3 matrix.

An analysis of the interfaces between possible coexisting phases 1 and 2 was carried out in terms of invariants of quadric surfaces [9, 10] $\sum_{a,b=1}^{3} D_{ab}x_a x_b = 0$, referenced in the Cartesian coordinate system $(X_1X_2X_3)$. The coefficients $D_{ab} = \sum_{f=1}^{3}(N_{af}^{(2)}N_{bf}^{(2)} - N_{af}^{(1)}N_{bf}^{(1)})$ can be given in terms of the elements of the distortion matrices $\|N_{af}^{(1)}\|$ and $\|N_{af}^{(2)}\|$ of phases 1 and 2, respectively. The shape of the interfaces separating these coexisting phases then depends on the following invariants [9, 10]:

$$I = D_{11} + D_{22} + D_{33}, \qquad D = \det\|D_{ab}\|$$
$$\text{and } J = \begin{vmatrix} D_{11} & D_{12} \\ D_{21} & D_{22} \end{vmatrix} + \begin{vmatrix} D_{22} & D_{23} \\ D_{32} & D_{33} \end{vmatrix} + \begin{vmatrix} D_{33} & D_{31} \\ D_{13} & D_{11} \end{vmatrix}. \tag{2}$$

It is obvious that the invariants from equations (2) depend on the unit-cell distortions of the coexisting phases and the volume fractions of the domain types therein. From the invariants we can identify real cone regions that correspond to various conical interfaces separating the coexisting phases, which obey the following inequalities: $DI < 0$ and $J < 0$ (designated as region I), $DI < 0$ and $J > 0$ (designated as region II), and $DI > 0$ and $J < 0$ (designated as region III). An additional imaginary cone apex is described by a fourth condition $DI > 0$ and $J > 0$ (region IV). Elastic matching between coexisting phases along so-called zero-net-strain planes (ZNSPs) obeys the following compatibility conditions:

$$DI = 0 \qquad \text{and} \qquad J < 0. \tag{3}$$

By achievement of conditions (3), the interfaces completely relax the stress, removing the excess elastic energy of the heterophase state. Below, we consider crystals obeying conditions (3) over a wide volume-fraction range of possible non-180° domain types (see figure 1) in the ferroelectric phases of PMN–0.30PT.

3. Domain state–interface diagrams

In our calculations, we used lattice parameters for PMN–0.30PT that were recently reported for $\boldsymbol{E} \parallel [111]$ over a wide temperature range [8]. According to x-ray data [8], changes in the lattice parameters were observed at temperatures of 403 K (C $\rightarrow$ T phase transitions), 371 K (T $\rightarrow$ O phase transition), and 350 K (O $\rightarrow$ $\mathrm{M_B}$ phase transition) on [111] field cooling. Due to a lack of experimental data for the monoclinic angle ($\beta_{\mathrm{M_B}}$) or the shear angle ($\omega_{\mathrm{M_B}} = 90° - \beta_{\mathrm{M_B}}$) as a function of temperature in the $\mathrm{M_B}$ phase, we assume the values of $\omega_{\mathrm{M_B}}$ to be in a range 0.04°–0.10°: these values are consistent with measured ones for PMN–xPT crystals with compositions close to the morphotropic phase boundary [7].

The coexistence of C–T phases in perovskite-type ferroelectric crystals is usually considered to be stabilized by the presence of two 90° domain types in the T phase, which provide complete stress accommodation in the heterophase state [10]. The volume fractions of the two types of 90° domains can be determined by zeroing-out the excess elastic energy via balancing spontaneous strains, unit-cell distortion, or electrostrictive contributions [10, 11, 13, 17] to the total strain from the various polydomain configurations. The results of our calculations for C–T phase coexistence are illustrated in the diagram shown in figure 2, where we balance the volume fractions of the 90° a- and c-domains (as denoted, for example, in monograph [11] and other works) in the T phase with regions of the C phase. The boundaries in this diagram separating regions I and III are dictated by the requirement

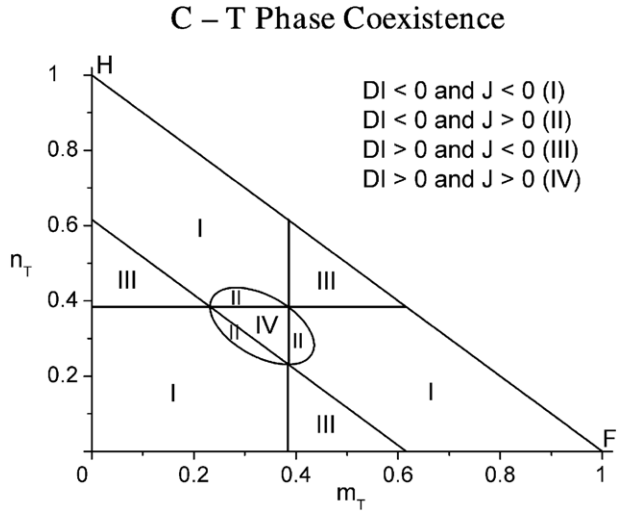

Figure 2. Domain state–interface diagrams for the C–T transition in field-cooled PMN–0.30PT crystals with a field of $E = 2$ kV cm^{-1} applied parallel to [111]. The polydomain T phase is described by the distortion matrix in equation (1*a*), the FH line obeys the condition $m_T + n_T = 1$ relating the volume fractions of the first and second domain types in the T phase.

that all interfaces be ZNSPs. The optimal volume fractions are ($m_T^{opt} = 0.384$ or 0.616) and ($n_T^{opt} = 0.616$ or 0.384). These values are in full compliance with the predictions based on formulae [10] for any two types of the 90° domains in the T phase. The lines defined by conditions $m_T = m_T^{opt}$ and $0 \leqslant n_T \leqslant n_T^{opt}$, or $n_T = n_T^{opt}$ and $0 \leqslant m_T \leqslant m_T^{opt}$, reflect the important role of two coexisting 90° domain types in stress relaxation. In fact, a third 90° domain type would slightly affect the balance of distortions in the polydomain crystals, because of the presence of two independent linear unit-cell distortions in each domain type; see elements ε_a and ε_c in matrices in equation (1*a*).

An interesting case of elastic matching occurs for T–O phase coexistence in PMN–0.30PT. It can be assumed that the volume fractions (m_T, n_T) of the 90° domains in the T phase correspond to lines separating regions I and III in figure 2 (i.e. as determined for the C–T transition) and that these volume fractions remain unchanged prior to the T–O phase transition. Such a stability of the 90° domain structure reflects an assumption that components of the $\boldsymbol{E}$ vector $E_i = E/\sqrt{3}$ are less than the coercive field of 90° reorientations in the T phase, over the temperature range between 403 and 371 K. Moreover, as the T phase becomes thermodynamically stable below 403 K, no driving force appears to change the balance of the volume fractions (m_T, n_T) which resulted from the *a priori* elastic matching of the C and T phases. A diagram represented in the (m_O, n_O) coordinate plane contains a few short lines that separate regions I and III (figure 3). These short lines correspond to different conditions satisfying the requirement that the T–O interfaces be ZNSPs. Independent of the values for (m_T^{opt}, n_T^{opt}) pairs, the conditions for ZNSPs (3) are fulfilled for the coexistence of polydomain T and near single-domain O phases. Strictly speaking, the inequalities $|OA| < 0.01$, $|OB| < 0.01$, $|CE| < 0.01$, $|CF| < 0.01$, $|GH| < 0.01$, and $|GK| < 0.01$ (see the various diagrams of figure 3) hold for all (m_T^{opt}, n_T^{opt}) points lying on boundaries between regions I and III in figure 2; accordingly, the formation of a single-domain O phase would result only in a slightly stressed state. Such favourable conditions for stress relaxation in PMN–0.30PT and the 'fine' structure of the diagrams in figure 3 for near single-domain O phase states stem from the following lattice parameter equality: $a_T = c_O$ [8].

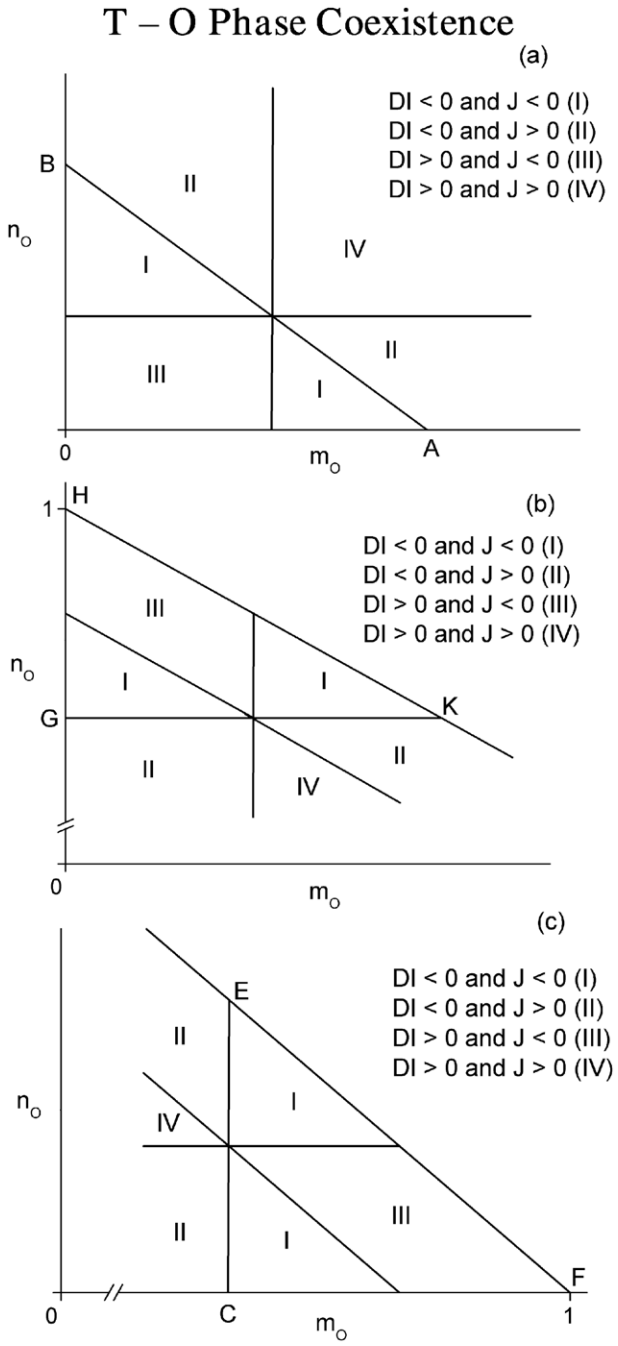

Figure 3. Domain state–interface diagrams for the T–O transition in [111] electric-field cooled PMN–0.30PT crystals. The polydomain T and O phases are described by the distortion matrices (1*a*) and (1*b*), respectively. The ZNSPs related to I–III boundaries are found in the vicinity of points $m_0 = n_0 = 0$ (see part a), $m_0 = 0$ and $n_0 = 1$ (see part b), and $m_0 = 1$ and $n_0 = 0$ (see part c). The HK and EF lines obey the condition $m_T + n_T = 1$ for the volume fractions of the first and second domain types in the O phase given by equation (1*b*).

Further cooling under $\boldsymbol{E} \parallel [111]$ results in an O–M_B transition. We now assume that the O phase is a single-domain state, characterized by one of the following distortion matrices:

$$\|N_{kl}^{(O,I)}\| = \begin{pmatrix} \eta_a & 0 & 0 \\ 0 & \eta_a & 0 \\ 0 & 0 & \eta_c \end{pmatrix}, \qquad \|N_{kl}^{(O,II)}\| = \begin{pmatrix} \eta_a & 0 & 0 \\ 0 & \eta_c & 0 \\ 0 & 0 & \eta_a \end{pmatrix}$$
$$\text{or } \|N_{kl}^{(O,III)}\| = \begin{pmatrix} \eta_c & 0 & 0 \\ 0 & \eta_a & 0 \\ 0 & 0 & \eta_a \end{pmatrix}. \tag{4}$$

Since the orientations of the spontaneous polarization vectors $\boldsymbol{P}_{Oj}$ of domains ($j = 1, 2, 3$) do not prefer one particular O relative to another, as $\psi_O(\boldsymbol{P}_{Oj}{}^{\wedge}\boldsymbol{E})$ is constant (see figure 1), one must then consider three possible different elastically matched O and M_B phase variants in PMN–0.30PT. Examples of corresponding diagrams interrelating domain states and interfaces are summarized in figure 4. These diagrams are simplified, relative to those shown for the T–O transition, because of the lattice parameter equalities $a_O = b_O = a_{M_B} = b_{M_B}$ previously reported at the O–M_B transformation [8]. Independent of the orientation of $\boldsymbol{P}_{Oj}$ (see figure 1 and equation (4)), the low-temperature M_B phase promotes the formation of ZNSPs over practically the entire range of n_{M_B} (see figure 4(a)) or m_{M_B} (see figures 4(b) and (c)) values. Of particular interest are the points ($m_{M_B} = 0$, $n_{M_B} = 1$) in figure 4(a) and ($m_{M_B} = 1$, $n_{M_B} = 0$) in figure 4(b), which correspond to single-domain M_B states that achieve coexisting single-domain O and M_B phases on [111] field cooling. Thus, a rotation of the spontaneous polarization vector [18] towards $\boldsymbol{E} \parallel [111]$ provides a simplification of the domain (twin) structures in the low-temperature phases.

It should be added that the O phase is observed as a single domain-like state [8], and that the probability of splitting this phase into non-180° domains is low. Moreover, favourable single-domain states in the O and/or M_B phase of PMN–0.30PT were accounted for by a redistribution of strain in the crystal sample [8], and the system of diagrams (see figures 3 and 4) is consistent with coexistence of both single-domain O and M_B phases at the first-order phase transition. This result could be of practical value in preparing single-domain relaxor–ferroelectric crystal samples on cooling under fairly weak electric fields.

4. Conclusions

In this work, relations between different domain (twin) structures and interfaces in polydomain/heterophase PMN–0.30PT crystals have been analysed for the case of electric-field cooling under $\boldsymbol{E} \parallel [111]$. We have summarized our results in a system of domain state–interface diagrams for a sequence of C $\rightarrow$ T $\rightarrow$ O $\rightarrow$ M_B transitions (figures 2–4). These diagrams show the various possibilities for achieving complete stress relaxation in systems with either coexisting C–T, T–O, or O–M_B phases. The planar interfaces regarded as ZNSPs appear in heterophase crystals due to favourable lattice parameter relations between coexisting phases and different non-180° polydomain states therein. Despite equal angles between the spontaneous polarization and applied $\boldsymbol{E}$ vectors (figure 1) in each of these phases, changes in the unit-cell parameters promote a simplification of the polydomain structures in coexisting O and M_B phases, that is as long as the angles $\psi_O(\boldsymbol{P}_{Oj}{}^{\wedge}\boldsymbol{E})$ and $\psi_{M_B}(\boldsymbol{P}_{M_Bj}{}^{\wedge}\boldsymbol{E})$ are considerably less than $\psi_T(\boldsymbol{P}_{Tj}{}^{\wedge}\boldsymbol{E})$ in the high-temperature T phase.

We believe that the approach developed in this work provides insights into (i) features of phase coexistence, (ii) domain (twin) structures in intermediate phases, and (iii) a correlation between some domain states and interfaces in heterophase PMN–xPT crystals under $\boldsymbol{E} \parallel [111]$. This approach is relevant for various ferroelectric and relaxor–ferroelectric crystals undergoing first-order phase transitions and exhibiting regular domain (twin) structures.

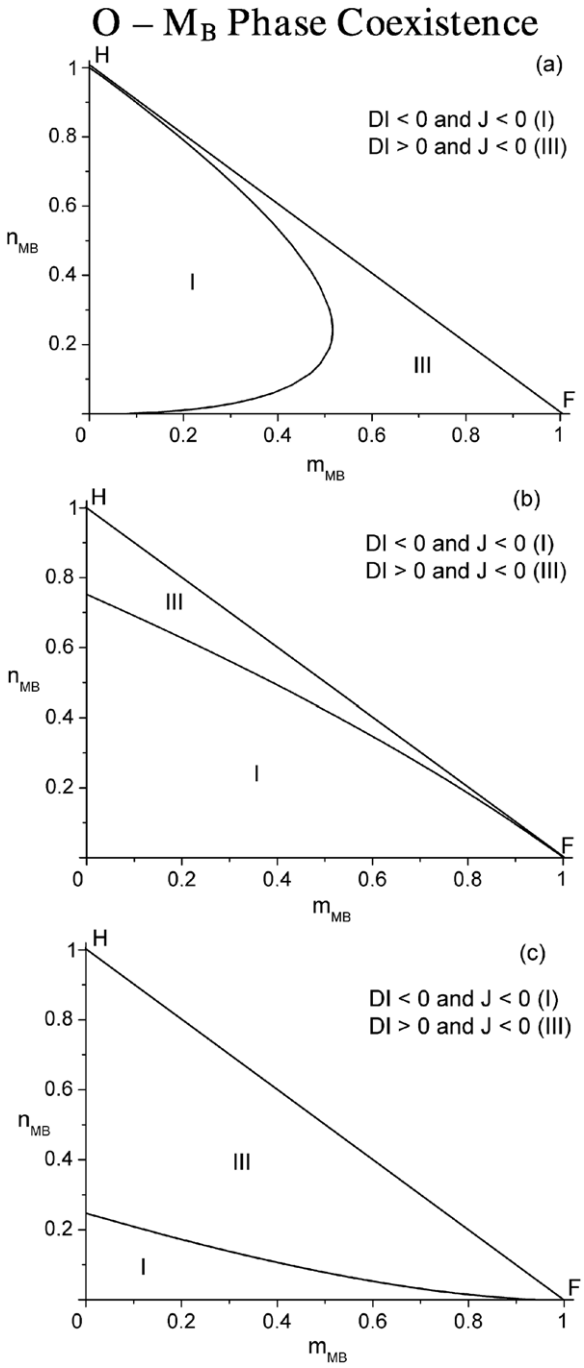

Figure 4. Domain state–interface diagrams for the O–M_B transition in [111] electric-field-cooled PMN–0.30PT crystals. The single-domain O phase is described by one of the distortion matrices of equations (4): i.e., $\|N_{kl}^{(O,I)}\|$ (see part a), $\|N_{kl}^{(O,II)}\|$ (see part b), and $\|N_{kl}^{(O,III)}\|$ (see part c). The polydomain M_B phase is described by the distortion matrix (1*c*). The FH line obeys the condition $m_{M_B} + n_{M_B} = 1$ for the volume fractions of the first and second domain types in the M_B phase given by equation (1*c*).

Acknowledgments

The authors thank Professors Z-G Ye (Canada), A V Turik and V G Gavrilyachenko (Russia) for their interest in the research problems. This work was partially supported by the administration of the Rostov State University (Southern Federal University since 2007, Project No. 11.1.06f on basic researches), and it is gratefully acknowledged by one of the authors (VYuT). Two of the authors (HC and DV) gratefully acknowledge the support of the Office of Naval Research (USA).

References

[1] Park S-E and Shrout T R 1997 *Mater. Res. Innov.* **1** 20
Zhang R, Jiang B and Cao W 2001 *J. Appl. Phys.* **90** 3471
[2] Noheda B, Cox D E, Shirane G, Gao J and Ye Z-G 2002 *Phys. Rev.* B **66** 054104
Singh A K and Pandey D 2003 *Phys. Rev.* B **67** 064102
Li J-B, Rao G H, Liu G Y, Chen J R and Liang J K 2004 *Ferroelectrics* **313** 71
[3] Topolov V Yu and Ye Z-G 2004 *Phys. Rev.* B **70** 094113
[4] Shuvaeva V A, Glazer A M and Zekria D 2005 *J. Phys.: Condens. Matter* **17** 5709
[5] Cao H, Li J, Viehland D and Xu G 2006 *Phys. Rev.* B **73** 184110
[6] Cao H, Bai F, Wang N, Li J, Viehland D, Xu G and Shirane G 2005 *Phys. Rev.* B **72** 064104
[7] Cao H, Li J, Viehland D, Xu G and Shirane G 2006 *Appl. Phys. Lett.* **88** 072915
[8] Cao H, Li J and Viehland D 2006 *J. Appl. Phys.* **100** 084102
[9] Topolov V Yu 2006 *Appl. Phys. Lett.* **89** 082904
[10] Topolov V Yu and Turik A V 1995 *Def. Diff. Forum Pt A* **123/124** 31
[11] Fesenko E G, Gavrilyachenko V G and Semenchev A F 1990 *Domain Structure of Multiaxial Ferroelectric Single Crystals* (Rostov-on-Don: Rostov University Press) (in Russian)
[12] Metrat G 1980 *Ferroelectrics* **26** 801
[13] Roytburd A L 1993 *Phase Trans.* B **45** 1
Roytburd A L 1974 *Sov. Phys.—Usp.* **17** 326
[14] Wechsler M S, Lieberman D S and Read T A 1953 *Trans. AIME, J. Met.* **197** 1503
Lieberman D S, Wechsler M S and Read T A 1955 *J. Appl. Phys.* **26** 473
[15] Abplanalp M, Barošová D, Bridenbaugh P, Erhart J, Fousek J, Günter P, Nosek J and Šulc M 2002 *J. Appl. Phys.* **91** 3797
Zeng H R, Yu H F, Hui S X, Li G R, Luo H S and Yin Q R 2006 *Mater. Sci. Eng.* B **127** 58
[16] Fousek J and Janovec V 1969 *J. Appl. Phys.* **40** 135
Bokov A A and Ye Z-G 2004 *J. Appl. Phys.* **95** 6347
[17] Topolov V Yu 2002 *Phys. Rev.* B **65** 094207
[18] Fu H and Cohen R E 2000 *Nature* **403** 281